Imaging characteristics of the Development Model of the SAX X-ray imaging concentrators.

O. Citterio, P. Conconi
Osservatorio Astronomico di Brera Merate - V. E. Bianchi 46-22055 Merate Italy

G. Conti, E. Mattaini, E. Santambrogio
CNR, Istituto di Fisica, Cosmica - V. Bassini 15-20133 Milano Italy

G. Cusumano, B. Sacco
CNR, Istituto di Fisica Cosmica - V. Stabile 172-90139 Palermo Italy

H. Brauninger, W. Burkert
Max Planck Institute für Extraterrestrische Physik - D-8046 Garching W. Germany

1.ABSTRACT

The imaging concentrators (4 units) are part of the payload of the italian satellite for X-ray astronomy SAX. They are operating in the energy range 0.3 - 10 Kev and have an angular resolution of 1 arcmin HPR. The effective area of each unit is 80 cm^2 at 2 Kev.
The optics is composed of 30 confocal nested very thin double cone mirrors.
To achieve a good optical quality and to allow the construction of several concentrators at an acceptable cost, a replica technique by electroforming the mirrors from masters is used.
To verify the thermomechanical and imaging properties of the optical system, a development model has been built having a set of 29 of the 30 mirrors. The mirrors are representative of the final ones except for the microroughness which is $\simeq$ 3 nm instead of $<$ 1 nm because, in order to have an earlier verification, they have been replicated from mandrels that have not yet been superpolished.
The optical system has been tested with low energy X-ray beam (E = 0.27 Kev) and with visible light. The results of these measurements are presented in the paper.

2.INTRODUCTION

The italian X-ray astronomy satellite SAX (1),(2),(3), has four imaging concentrators onboard operating in the 0.3 - 10 KeV energy range with a design goal of 1 min of arc half power radius (HPR) for angular resolution. The effective area of each unit is 80 cm^2 at 2 KeV and 44 cm^2 at 7 KeV. The focal length is 1.85 m.
Each unit is composed of thirty nested coaxial and confocal mirrors having thicknesses ranging from 0.2 to 0.4 mm respectively for the innermost and outermost mirrors. The diameters of the mirrors range between 55 and 147 mm while the overall length is 300 mm for all the mirrors.

The weight of each imaging concentrator (set of thirty mirrors plus the support structure) is 13 Kg.
Considering the large number of mirror units needed for the qualification and flight models of the SAX program and the stringent requirements for angular resolution and thickness of the mirrors wall, a replica technique by nickel electroforming the mirrors from mandrels was considered as the most appropriate for making the SAX optics.
The microroughness of the mandrels must be better than 1 nm rms.
The design of the optics was published in a previous paper (4). For the geometry of the optics a double cone approximation of the Wolter I profile was identified as the best trade-off between the manufacturing cost of the mandrels and the angular resolution, which is ultimately limited by the spatial resolution of the gas proportional counter (GSPC) envisaged for the focal plane.
The characterisation of the innermost and outermost of the set of thirty mirrors was presented in a previous paper (5).
Here we report the imaging properties of the Development Model (D.M.) of the SAX imaging concentrator, which has a set of 29 of the 30 mirrors.

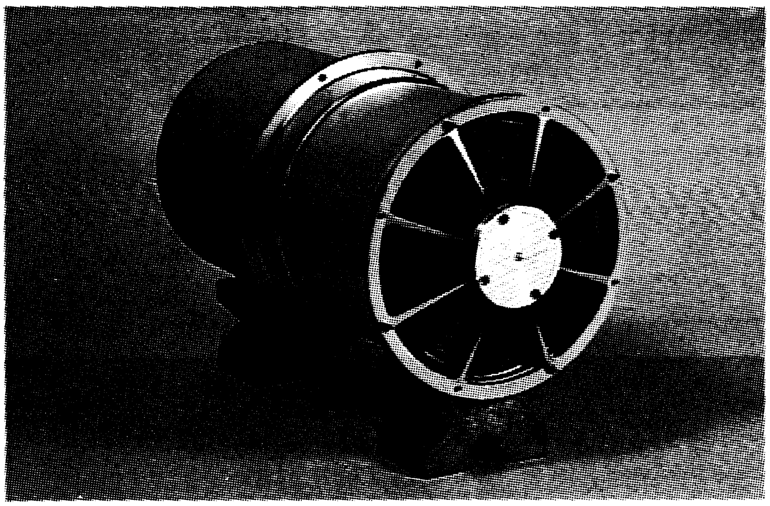

Fig. 1 - Developmente Model (D.M.) of the SAX imaging concentrator

The D.M., which is shown in Fig.1, was built to verify the thermomechanical and the imaging quality of the optical system.
The mirrors are representative of the final ones except for the microroughness which is $\simeq 3$ nm instead of the required < 1 nm because, in order to have an earlier verification in the SAX program, they were replicated from mandrels that were not yet superpolished.
The optical system was tested with a low energy X-ray beam (E= 0,27 KeV) in order to make an assesment of the image quality of the optical system, almost indipendently of the scattering effects.
The optical system was also tested with visible light; this measurement provides a

quick and easy way of making an assesment of the aberrations of the optics. The results from visible and X-ray measurements are reported and compared in the paper.

3.X-RAY MEASUREMENTS

The X-ray test of the D,M. was performed at the PANTER facility (6) of Max Planck Institute in Munich.
Fig. 2 shows the D.M. mounted in the vacunm chamber; the optical bench can be horizontally and vertically tilted with respect to the X-ray beam. On the left-hand side of the figure, three types of detectors are visible: 1) an imaging microchannel plate detector (MPC), 2) a proportional counter having a 150 μm width slit, and 3) a proportional counter with a diameter of 23 mm.

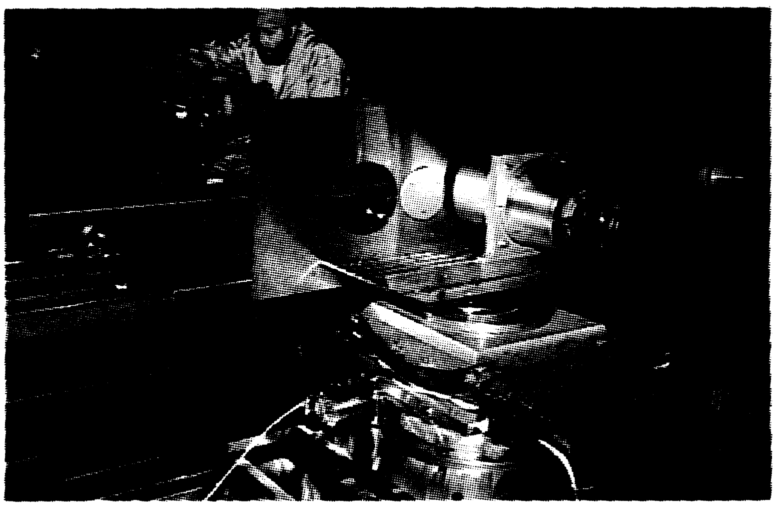

Fig. 2 - The D.M. mounted inside the PANTER X-ray test facility

The spatial resolution of the MCP detector is 80 μm which corresponds, to our focal length, to an angular resolution of 8.9 arcsec.
The detectors can be horizontally and vertically translated and also moved along the optical axis to find the best focus position. A proportional counter is also mounted in the beam to monitor possible fluctuations of the intensity of the beam.
For the imaging test we used the MCP detector.
The useful aperture of the mirrors is illuminated by an X-ray beam coming from a pointlike source 130 m away. The resultant divergence of the beam is 1.5 and 3.9 arcmin, respectively, for the innermost and outermost mirrors.
The results that follow are corrected by ray tracing to bring the source to infinity.
The purpose of the X-ray measurements of the D.M. was to verify the imaging quality of the mirrors module in order to determine if the manufacturing processes adopted were able to fulfil the SAX requested specification of an HPR $\leq$ 1 arcmin.
The measurements were made at 0.27 KeV (Carbon line) to minimize the contribution of the scattering effects to the image quality.

This situation allow us to make an assesment of the overall aberrations that are generated during the manufacturing processes.

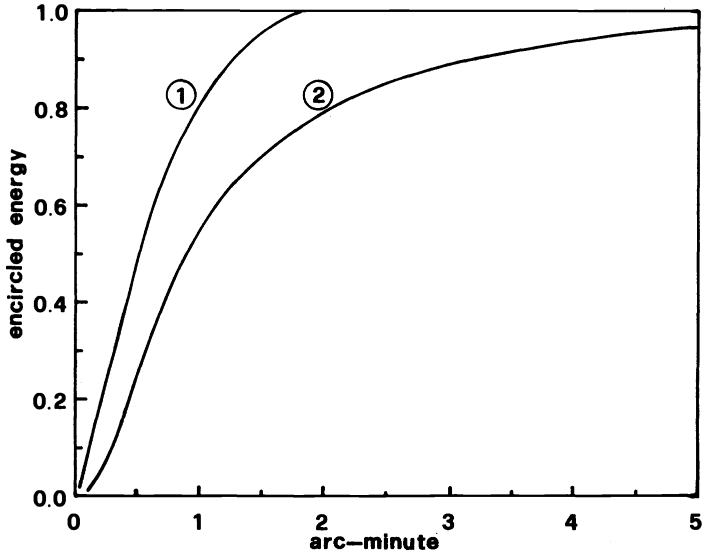

Fig. 3 - Intrinsic (curve 1) and measured (curve 2) Encircled Energy function for the D.M. of the SAX imaging concentrator

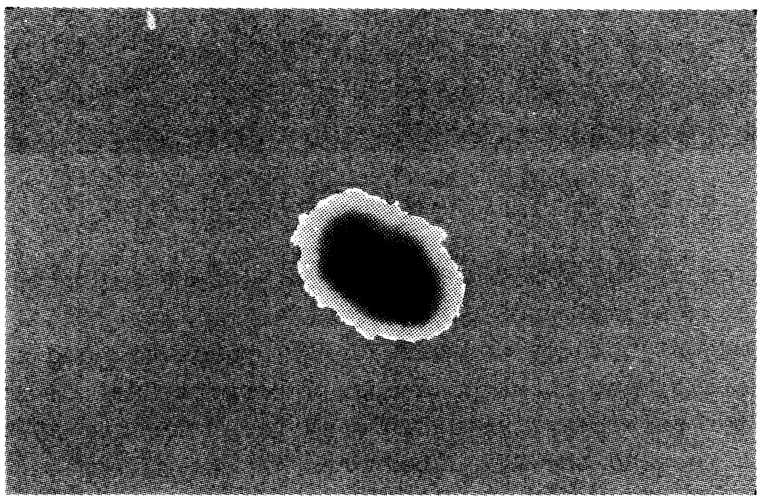

Fig. 4 - D.M. of the SAX imaging concentrator; two equal intensity sources separated by 60 arcsec at 0.27 KeV

These are:

1) manufacturing errors of the mandrels (deviation from a perfect double cone)
2) errors generated during the electroforming process (possible internal stress effects)
3) manufacturing errors of the two supporting spider structure (deviation from

nominal diameter and out of roundness of the spider grooves)
4) errors generated during the assembly of the mirrors into structure.
5) error due to gravity effects.

Fig.3 shows the intrinsic encircled energy function of a SAX imaging concentrator calculated by ray tracing (curve 1) and the one measured at 0.27 KeV for the D.M. (curve 2). The HPR values are respectively 30 arcsec and 52 arcsec.
Fig. 4 shows two equal intensity sources separated 60 arcsec, simulated at the PANTER facility. The picture is a black-and-white reconstitution of a color photograph of the MCP image presented on a color TV screen. The contrast of the image is enhanced by software.

In table I are computed which would be the values of the HPR for the D.M. at 5 and 8 KeV taking into consideration also the effects of the microroughness of the reflecting surfaces. The computation has been done using a microroughness model which best fit the measurements made on two samples of superpolished SAX mirrors. Three values of microroughness are taken as reference: 0.5, 0.75 and 1 nm.

Microroughness (nm)	HPR at 5 Kev (arcsec)	HPR at 8 KeV (arcsec)
0.50	56	58
0.75	59	70
1.00	65	94

Table I - Computed HPR values for the D.M. at 5 and 8 KeV considering three different values of microroughness

A verification of the actual diameter of the grooves on both spiders, after the X-ray measurements, has shown a systematic error of these diameters introduced during machining of the spiders. The errors have been corrected and a new X-ray test of the D.M. was made. The new measurements have given a value of 41 arcsec for the HPR. By computing the effects of the scattering at 5 and 8 KeV we obtain the values of HPR given in Table II.

Microroughness (nm)	HPR at 5 KeV (arcsec)	HPR at 8 KeV (arcsec)
0.50	46	49
0.75	50	62
1.00	57	88

Table II - Computed HPR values for the D.M. after the correction of the diameters of the spider grooves, at 5 and 8 KeV.

4.MEASUREMENTS WITH VISIBLE LIGHT

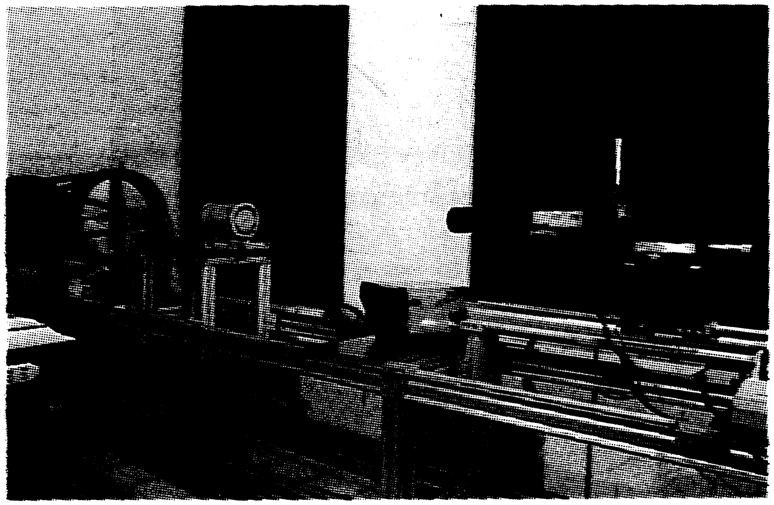

Fig. 5 - Optical bench for the measurements of the mirror shells with visible light

The measurements with visible light provide a quick and easy way of making a first assesment of the image quality of the mirrors; consequently is very convenient to have a testing facility operating with visible light during the manufacture of the mirrors and during their integration into the mechanical supporting structure. Of course with these visible measurements is not possible to make an assesment on the microroughness of the reflecting surfaces. The measurements were made on the optical bench which is shown in Fig. 5.

The aperture of the optical system is fully illuminated by a beam of parallel light coming from a collimator which operate with a He Ne laser source (λ = 633 nm).

At the focal plane the image is analized either by a CCD camera or by means of a silicon detector with a slit in front, which can make a scan across the image, giving its line spread function.

From the measurements with visible light, the Encircled Energy (EE) function is derived. This EE is strongly affected by the diffraction of the light, occuring at this wavelength. In order to derive the X-ray EE it is necessary to correct for the effects of the diffraction because these are negligible at X-ray wavelengths.

For making this correction we use the Modulation Transfer Function (MTF) of our optical system as described for example in (7). Dealing with the MTF, we make the assumption of considering only simmetric aberrations.

The relationship between the EE and MTF is given by (8):

$$EE(w) = 2\pi w \int_0^1 T(\nu_n) J_1(2\pi \nu_n w)\, d\nu_n \qquad 1$$

where $w = \alpha D/\lambda = \alpha \nu_c$, α is the angular radius of the image, D is the diameter of the optics, λ is the wavelength, ν_c is the cutoff frequency $\nu_c = D/\lambda$, J_1 is the first

order Bessel function and ν_n is the normalized spatial frequency.
In our calculations we consider the MTF composed of the following factors:

$$T = Td\ Tf\ Tr \qquad 2$$

where T = MTF of the optical system
Td= MTF for a perfect system (diffraction effects)
Tf= degradation function due to the conical approximation
Tr= degradation function due to random wavefront variation arising from errors of the mandrel polishing process, spider fabbrication, mirrors integration.
For the degradation function Tr we assume the form derived by O'Neill(9) which is:

$$T_r = \exp\left\{-k^2\omega^2\left[1-c(\nu_n)\right]\right\} \qquad 3$$

Where $k = 2\pi/\lambda$, ω is the RMS random wavefront error and $c(\nu_n)$ is the normalized autocorrelation function of the residual pupil function.
The $c(\nu_n)$ modeled as a Gassian has the form:

$$c(\nu_n) = \exp\left(-4\nu_n^2/\ell^2\right) \qquad 4$$

The parameter ℓ is called the correlation length and is a measure of the structures on the wavefront.
In our case we consider 4 correlation lengths having a spatial period corresponding to 1/2, 1/3, 1/4 and 1/5 of the length of one cone of a mandrel, which we consider most likely to occur during the manufacturing process of the mandrels; by means of a best fit process, 4 values of ω_n are derived that, through the 1,2 and 3, best represent the measured EE.
As an example, Fig. 6 and Fig. 7 show the correspondence between the measured E.E. and the computed EE for the SAX mirror shells 9A and 22A.
In order to calculate the equivalent slope error values of the mirror profile, from the ω_n and ℓ_n values of the wavefront, the following relation is used

$$\alpha_n = \mathrm{arctg}\left(q\,\omega_n\lambda/\ell_n\right) \qquad 5$$

where α_n = rms slope error and q is a constant which is defined by means of a autoregressive process of order m, such to obtain the same rms on the wavefront and the same $c(\nu_n)$ in m points. In our case q = 2.6.

To derive the X-ray EE we now apply to the photon propagation, four Gaussian distribution each having a zero average value and an rms α_1, α_2, α_3, and α_4. Considering the spot diagram obtained by ray tracing of 20000 rays, the X-ray EE is calculated.

In order to verify our approach we checked its validity on four SAX single mirror shells for which the measurements with visible light and with X-ray photons, were available.

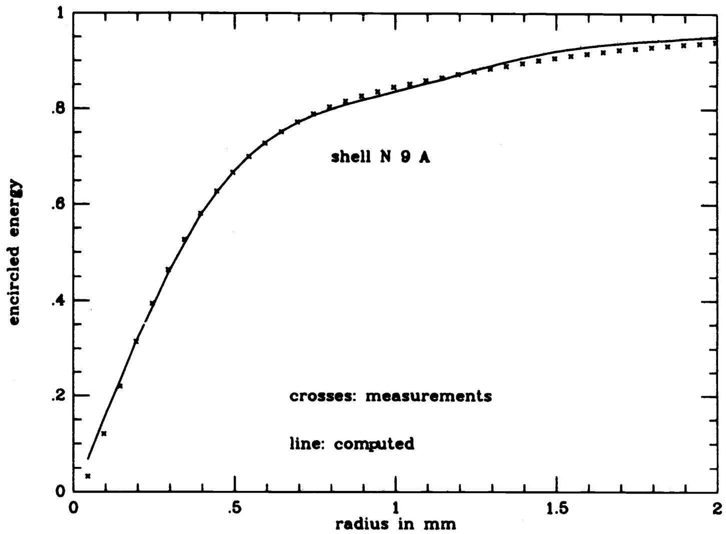

Fig. 6 - Comparison between computed and measured Encircled Energy function for SAX mirror shell 9A

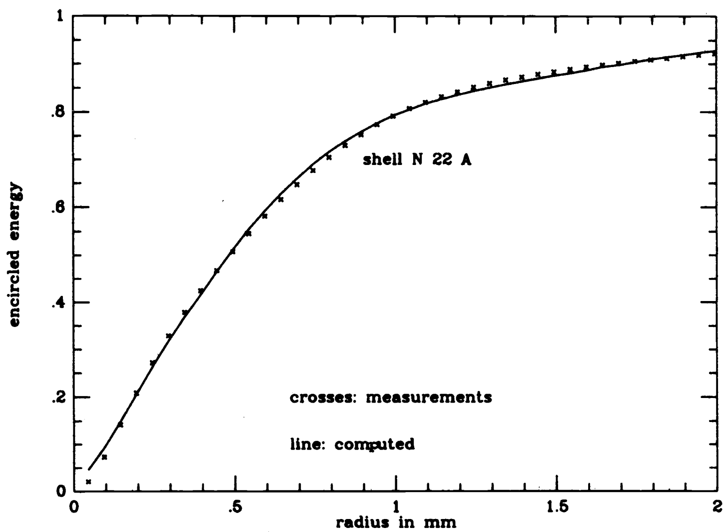

Fig. 7 - Comparison between computed and measured Encircled Energy function for SAX mirrors shell 22A

The results are shown in Table III. The agreement between HPR predicted from the measurements in the visible and the ones measured with X-ray photons is within ± 10%.

Mirror Shell	HPR1 Measured with visible light (arcsec)	HPR2 X-ray predicted from visible measurements (arcsec)	HPR3 X-ray measurements (arcsec)	$\frac{HPR2-HPR3}{HPR3}$ %
9 A	36	44	48	- 8
9 B	32	36	38	- 5
22 A	54	50	50	0
22 B	49	49	44	+10

Table III. Comparison between the HPR predicted from measurements in the visible and the ones measured with X-ray photons.

For the D.M. each mirror shell was measured in the visible applying a serie of 29 aperture stops on the entrance aperture of the mirror unit; from the measurements with visible light the predicted X-ray EE of each mirror shell were calculated. Combining these EE functions by giving a weight which is dependent on the effective area of each mirror shell, the predicted X-ray HPR for the whole mirrors module was computed. The derived value is 53 arcsec, which compares pretty well with the value of 52 arcsec obtained from direct X-ray measurements of the complete mirrors module.
The evaluation of the image quality with visible light was not made on the D.M. after the correction of the diameters of the spider grooves.

5.CONCLUSIONS

The results of the X-ray measurements made on the D.M. of the SAX imaging concentrators, shown in Table II, indicate that the manufacturing process chosen is capable of fulfilling the design specification of HPR ≤ 60 arcsec, provided that the microroughness of the mirrors is kept below 0.75 nm. Values of microroughness ≤ 0.75 nm have been normally obtained on samples of superpolished SAX mirrors.
The measurements with visible light provide a convenient way of making a first assessment of the image quality of the mirrors; the approach followed to predict the X-ray EE from one measured with visible light provide results that are in good agreement with the real X-ray measurements.

ACKNOWLEDGMENTS

The electroformed mirrors were provided by Elettroformatura TENCA - Milano; the machining of the spider grooves by electron discharge machining were made by STEMA - Ciserano while the mandrels were supplied by MACDIT - Lecco. BCV - Milano has made the static and dynamic calculations of the mirror module. We wish to thank U.

Bergamini and L. Valtolina for the mechanical measurements on two spider systems and on the set of mirror shells.
Finally we like to thank Prof. G. Boella, C. Perola and L. Scarsi for encouraging and supporting this work.

6.REFERENCES

1. L. Scarsi, "The SAX mission", Adv. Space Res., N. 10-12 - 500, 1984.
2. G. Spada, "SAX Scientific Instrumentation", Proceedings of "Non thermal and very high temperature phenomena in X-ray Astronomy", pp 217-234, Rome 1983.
3. C. Perola, "The scientific objectives of the SAX mission", Proceedings of "Non thermal and very high temperature phenomena in X-ray Astronomy", pp 173-230, Rome 1983.
4. O. Citterio, G. Conti, E. Mattaini, B. Sacco, E. Santambrogio, "Optics for X-ray concentrators on board of the Astronomy Satellite SAX", SPIE vol 597 - X-ray instrumentation in astronomy, 1985.
5. O. Citterio, G. Bonelli, G. Conti, E. Mattaini, E. Santambrogio, B. Sacco, E. Lanzara, H. Brauninger, W. Burkert, "Optics for the X-ray imaging concentrator aboard the X-ray astronomy satellite SAX", Ap. Op. vol. 27, N. 8, 1470, 1988.
6. B. Aschenbach, H. Brauninger, K.H. Stephan, J. Trumper, "X-rays test facilities at Max Planck Institut Garching", SPIE vol 184 - Space Optics-Imaging X-ray optics Workshop, 1979.
7. D.J. Schroeder, "Astronomical Optics", Academic Press Inc., 1987, Chapter 10 and 11.
8. Ibidem, pag. 204.
9. Ibidem, pag. 208.